SOLVATION DYNAMICS AND VIBRATIONAL RELAXATION IN RESONANCE RAMAN AND FLUORESCENCE LINESHAPES OF TETRADESMETHYL-β-CAROTENE

James SUE, Shaul MUKAMEL [1]
Department of Chemistry, University of Rochester, Rochester, NY 14627, USA

Hiromi OKAMOTO [2], Hiro-o HAMAGUCHI and Mitsuo TASUMI
Department of Chemistry, Faculty of Science, University of Tokyo, Bunkyo-ku, Tokyo 113, Japan

Received 7 October 1986; in final form 24 November 1986

We report the measurements and microscopic theoretical analysis of resonance fluorescence and Raman lineshapes of tetradesmethyl-β-carotene in isopentane at 190 and 230 K. We find the solvent correlation time to be 125 fs at 190 K, 111 fs at 230 K and the vibrational relaxation time to be 253 fs at both temperatures. The dependence of the Raman yield on the solvation dynamics and the detuning is predicted.

1. Introduction

The spontaneous emission lineshapes of large polyatomic molecules in solution often consist of progressions of sharp lines (Raman), accompanied by relatively diffuse lineshapes (fluorescence) [1–5]. Similar behavior is found in near resonance excitation of molecules in the gas phase [6,7], in supersonic beams [8] and molecular crystals [9]. The absorption lineshapes of solvated molecules are usually smooth and relatively featureless yielding little microscopic information, whereas the Raman lines and their excitation profiles may be used to extract structural constants (vibrational frequencies and nuclear displacements) as well as line broadening parameters. Considerably less attention is usually given to the fluorescence component. Its measurement requires careful calibration and the elimination of other sources of background emission, and its theoretical interpretation is less straightforward. However we have recently shown [7,10] how a careful analysis of the fluorescence lineshapes may provide extremely useful additional information regarding the solvation dynamics and vibrational relaxation (VR) rates. In particular the relative intensity of the Raman and fluorescence components and its variation with detuning provides a direct probe for the solvent time scales and allows a convenient distinction between homogeneous and inhomogeneous broadening mechanisms. In this Letter we report detailed measurements of fluorescence and the Raman spectra of tetradesmethyl-β-carotene (19,19′,20,20′-tetranor-β,β-carotene, TNBC) in isopentane at 190 and 230 K. A theoretical analysis based on our microscopic model [7,10] allows us to interpret the fluorescence lineshapes and the individual Raman yields. The solvent correlation time, the magnitude of the solvent-molecule interactions and the VR rate are obtained from our analysis.

2. Experimental

Spectral measurements were performed with a Raman spectrometer consisting of a NEC Ar^+ laser (GLG 3300) and a NEC He–Cd laser (GLG 2018), a Spex monochromator (modified for computer control), a

[1] Camille and Henry Dreyfus Teacher–Scholar.
[2] Present address: Institute for Molecular Science, Myodaiji, Okazaki 444, Japan.

0 009-2614/87/$ 03.50 © Elsevier Science Publishers B.V.
(North-Holland Physics Publishing Division)

Hamamatsu R-649 photomultiplier and a photon counter. An Oxford cryostat DN704 was employed for low-temperature measurements. The Ar^+ laser lines at 501.7, 496.5, 488.0, 476.5, 472.7, 465.8 and 457.9 nm, and the He–Cd laser line at 441.6 nm were used for excitation. The spectrometer sensitivity correction was made using the data based on the intensities of the rotational Raman bands of H_2 and D_2 [11]. The bands of isopentane (solvent) at 790, 1450 and 2860 cm^{-1} were used as the internal intensity reference. The experimental results were obtained at the University of Tokyo.

3. The microscopic model

The major problem in the microscopic analysis of spontaneous emission lineshapes of polyatomic molecules in condensed phases arises from the large number of degrees of freedom which should be incorporated in the calculation. A large molecule has many vibrational modes; these are partitioned into a set of a few relevant optically active modes (i.e. those with large Franck–Condon factors) which form the molecular "system" and a set of inactive (dark) modes. These latter modes together with the solvent constitute a thermal "bath" which interacts with the molecular system, causing spectral broadening and inducing the fluorescence component. In principle the spontaneous emission lineshapes may be calculated using the Kramers–Heisenberg (KH) formula [2,4] provided all degrees of freedom (system and bath) are incorporated explicitly in the calculation. This requires the complete knowledge of the molecular and the solvent eigenstates which is impractical for realistic condensed phase systems. Moreover, the molecular spectra are not sensitive to the detailed eigenstates of the solvent so that even if a KH calculation were feasible it would end up averaging most of the solvent microscopic information. A complete KH calculation of spontaneous emission lineshapes in solution is therefore neither feasible nor desirable and in view of these considerations, it is obvious that a *reduced description* of the process is more appropriate. Such a reduced description should be based on reduced equations of motion which contain the system degrees of freedom explicitly and the effects of the bath are incorporated in an averaged way via relaxation and dephasing processes. A reduced description requires reformulating the problem using the density matrix in Liouville space [7,10]. The KH formula does not apply any longer within a reduced description and we cannot write the spontaneous emission lineshapes as the square of an amplitude. We shall now introduce our microscopic model which provides a reduced description of spontaneous emission lineshapes in large molecules.

We consider a polyatomic molecule with N optically active vibrational modes and two electronic states, the ground state $|g\rangle$ and the excited state $|e\rangle$. The molecular Hamiltonian is

$$H = |g\rangle H_g \langle g| + |e\rangle [H_e + \omega_{eg} + \delta\omega_{eg}(t)] \langle e| \,. \tag{1a}$$

H_g (H_e) is the nuclear Hamiltonian of the electronic ground (excited) state. Adopting a harmonic model for the vibrational modes and setting $\hbar = 1$, we have

$$H_g = \tfrac{1}{2} \sum_{j=1}^{N} \omega_j'' (p_j''^2 + q_j''^2 - 1) \,, \tag{1b}$$

$$H_e = \tfrac{1}{2} \sum_{j=1}^{N} \omega_j' (p_j'^2 + q_j'^2 - 1) \,, \tag{1c}$$

where ω_j' and ω_j'' are the vibrational frequencies of mode j; q_j' and q_j'' are the dimensionless nuclear coordinates related by the transformation

$$q_j' = (\omega_j'/\omega_j'')^{1/2} q_j'' + d_j \tag{2}$$

and d_j is the dimensionless displacement of mode j. ω_{eg} is the average electronic energy gap (0–0 transition).

Our reduced description of the bath is based on the assumption that the molecular interactions with the solvent and the optically inactive vibrational modes of the molecule introduce a stochastic modulation $\delta\omega_{eg}(t)$ of the electronic energy gap. We assume $\delta\omega_{eg}(t)$ to be a Gaussian Markovian process with zero mean, $\langle\delta\omega_{eg}(t)\rangle=0$, and its correlation function is [7,10]

$$\langle\delta\omega_{eg}(t)\ \delta\omega_{eg}(0)\rangle=\Delta^2\exp(-\Lambda t)\ . \tag{3}$$

Δ is the magnitude of the stochastic modulation and Λ is its inverse correlation time. We find it useful for the subsequent discussion to introduce two alternative parameters, κ and Γ_0. $\kappa\equiv\Lambda/\Delta$ measures the modulation rate relative to its magnitude. In the fast modulation limit ($\kappa\gg 1$), the broadening is homogeneous whereas in the slow modulation limit ($\kappa\ll 1$), the broadening is inhomogeneous. Γ_0 is the full width at half maximum of the broadening induced in the absorption lineshape (i.e. Im $J_0(\omega)$, eq. (9)) by the interaction with the solvent [10]

$$\Gamma_0/\Delta\approx(2.355+1.76\kappa)/(1+0.85\kappa+0.88\kappa^2)\ . \tag{4}$$

The molecular density matrix ρ evolves in time according to the Liouville equation

$$\mathrm{d}\rho/\mathrm{d}t=-\mathrm{i}\,L\rho-\Gamma\rho\ , \tag{5a}$$

where

$$L\rho\equiv[H,\rho] \tag{5b}$$

and Γ is a phenomenological damping matrix introduced to account for vibrational relaxation and radiative lifetime of the electronic excited state [7,12]. Consider two vibronic levels $|b\rangle$ and $|d\rangle$ belonging to the electronic excited state with energies E_b and E_d and radiative lifetime $(\gamma^r)^{-1}$. The matrix element $\langle\langle dd|\Gamma|bb\rangle\rangle$ represents the vibrational relaxation rate from level $|b\rangle$ to level $|d\rangle$. Like any master equation, Γ satisfies detailed balance

$$\langle\langle dd|\Gamma|bb\rangle\rangle=\langle\langle bb|\Gamma|dd\rangle\rangle\exp(-\omega_{db}/kT)\ , \tag{6a}$$

with $\omega_{db}=E_d-E_b$. The total decay rate of level $|b\rangle$, γ_b, is given by

$$\gamma_b=-\sum_{d\neq b}\langle\langle dd|\Gamma|bb\rangle\rangle+\gamma^r\ . \tag{6b}$$

In addition we have

$$\langle\langle bd|\Gamma|bd\rangle\rangle=\tfrac{1}{2}(\gamma_b+\gamma_d)\ . \tag{6c}$$

All other matrix elements of Γ not specified in eqs. (6a)–(6c) are zero. In the following calculations we have adopted the simplest relaxation scheme and assumed that all vibronic states $|b\rangle$ relax to the ground vibrational state $|0\rangle$ within the electronic excited state with the same rate γ^v and that all matrix elements $\langle\langle dd|\Gamma|bb\rangle\rangle$ for $d\neq 0$ vanish, i.e.

$$\langle\langle dd|\Gamma|bb\rangle\rangle=-\gamma^v\delta_{d,0}\ . \tag{6d}$$

In a frequency-domain spontaneous emission experiment the molecule absorbs a photon ω_L and emits a photon ω_S. The total spontaneous emission lineshape is given by [7,10]

$$S(\omega_L,\omega_S)=S_F(\omega_L,\omega_S)+S_R(\omega_L,\omega_S)+S_{BR}(\omega_L,\omega_S)\ , \tag{7a}$$

where we have partitioned the emission into three components: fluorescence, $S_F(\omega_L,\omega_S)$; sharp Raman $S_R(\omega_L,\omega_S)$; and broad Raman, $S_{BR}(\omega_L,\omega_S)$, where

$$S_F(\omega_L,\omega_S)=-i\omega_L\omega_S^3\sum_{n=0}^{\infty}\frac{1}{n!\kappa^{2n}}\sum_{a,b,c,d}P(a)J_n(\omega_L-\omega_{ba}+\tfrac{1}{2}i\gamma_b)$$

$$\times\Bigg[\mu_{cb}\mu_{ba}\mu_{ad}\mu_{dc}\left(\frac{(\delta_{bd}-1)^nJ_n(\omega_S-\omega_{bc}+\tfrac{1}{2}i\gamma_b)+(1-\delta_{bd})J_n(\omega_{dc}-\omega_S+\tfrac{1}{2}i\gamma_d)}{\omega_{db}+i(\tfrac{1}{2}\gamma_b+\tfrac{1}{2}\gamma_d+n\Lambda)}\right.$$

$$\left.+\mathrm{PP}\frac{J_n(\omega_{dc}-\omega_S+\tfrac{1}{2}i\gamma_d)}{\omega_L-\omega_S-\omega_{ca}+in\Lambda}\right)$$

$$-i|\mu_{ab}|^2|\mu_{dc}|^2\ll dd|(\Gamma+n\Lambda)^{-1}|bb\gg[J_n(\omega_{dc}-\omega_S+\tfrac{1}{2}i\gamma_d)-(-1)^n\mathrm{c.c.}]\Bigg]+\mathrm{c.c.}\,, \tag{7b}$$

$$S_R(\omega_L,\omega_S)=2\pi\omega_L\omega_S^3\sum_{a,c}P(a)|K_{ca}(\omega_L)|^2\delta(\omega_L-\omega_S-\omega_{ca})\,, \tag{7c}$$

$$S_{BR}(\omega_L,\omega_S)$$

$$=i\omega_L\omega_S^3\sum_{a,c}P(a)\sum_{n=1}^{\infty}\frac{1}{n!}K_{ca}^{(n)}(\omega_L)K_{ca}^{(n)*}(\omega_S+\omega_{ca})\frac{n\Lambda}{(\omega_L-\omega_S-\omega_{ca})^2+(n\Lambda)^2}+\mathrm{c.c.} \tag{7d}$$

and

$$K_{ca}^{(n)}(\omega)=\frac{1}{\kappa^n}\sum_b\mu_{cb}\mu_{ba}J_n(\omega-\omega_{ba}+\tfrac{1}{2}i\gamma_b)\,, \tag{7e}$$

$$K_{ca}(\omega)\equiv K_{ca}^{(0)}(\omega)\,. \tag{7f}$$

The corresponding expression for the absorption lineshape is given by

$$\sigma(\omega_L)=-2\omega_L\sum_{a,b}P(a)|\mu_{ba}|^2\,\mathrm{Im}\,J_0(\omega_L-\omega_{ba}+\tfrac{1}{2}i\gamma_b)\,. \tag{8}$$

In eqs. (7) and (8), a and c denote vibronic levels belonging to the ground electronic state and b, d denote vibronic levels belonging to the electronic excited state. $P(a)$ is the equilibrium population of level a, μ is the electronic dipole moment which is taken to be independent of the nuclear coordinates (the Condon approximation) and its matrix elements are proportional to the Franck–Condon factors [13]. PP represents the principal part and $J_n(s)$ are the lineshape functions

$$J_n(s)=-i\int_0^{\infty}d\tau\,[1-\exp(-\Lambda\tau)]^n\exp[is\tau-g(\tau)]\,, \tag{9a}$$

wnere

$$g(\tau)=(\Delta^2/\Lambda^2)[\exp(-\Lambda\tau)-1+\Lambda\tau)]\,. \tag{9b}$$

The broad Raman component, $S_{BR}(\omega_L,\omega_S)$, consists of a series of progressively broader lineshapes centered around the Raman lines at $\omega_L-\omega_S=\omega_{ca}$, having widths of $n\Lambda$. Typically, in solution, Λ is of the order of 100 cm^{-1} so that S_{BR} will contribute to the fluorescence component [10]. However when Λ is very small, $\Lambda\sim\gamma^r$, S_{BR} may contribute to the Raman component. In the present article we incorporate S_{BR} in the fluorescence component. It should be noted that the KH expression for Raman [5] is identical with S_R (eq. (7c)) in the limiting case whereby $\Lambda\gg\Delta$ and $g(\tau)=\Delta^2/\Lambda$. The KH expression does not contain the other components (S_F and S_{BR}). The last term in eq. (7b) represents VR from level b to level d for $b\neq d$ and depends primarily on the ratio $\alpha\equiv\gamma^v/\gamma^r$. When $\alpha\gg1$, the vibronic levels of the excited state very quickly reach thermal equilibrium and the emission is fully relaxed [7,12]. In the opposite limit, $\alpha\ll1$, the VR does not affect the emission spectrum.

We shall also introduce the absolute individual Raman yield. This is defined as the integrated cross section of the Raman line at $\omega_L - \omega_S = \omega_{ca}$ divided by the absorption cross section. It is given by

$$Y_{ca}(\omega_L) = \frac{4\omega_L \omega_S^3}{3C^3} \frac{|K_{ca}(\omega_L)|^2}{\sigma(\omega_L)}, \tag{10}$$

where C is the speed of light. The Raman yield is readily available experimentally and provides a sensitive indicator for the magnitude of κ [14].

4. Results

TNBC has two active Raman modes [5] with ground state frequencies $\omega_1'' = 1523\ \text{cm}^{-1}$ and $\omega_2'' = 1133\ \text{cm}^{-1}$. In the top two panels in fig. 1 we display the experimental absorption spectra of TNBC at 230 and 190 K together with our calculations (eq. (8)) which are in excellent agreement. The Raman yield $Y_{ca}(\omega_L)$ (eq. (10)) provides a direct probe for κ. In the lower three panels in fig. 1 we display our experimental (solid circles) and calculated relative Raman yield for our best fit ($\kappa = 0.1$) of the 190 K lineshapes. In addition we repeated these calculations for different values of κ ($\kappa = 1$ and 10) keeping the same value of Γ_0. The sensitivity of the yield

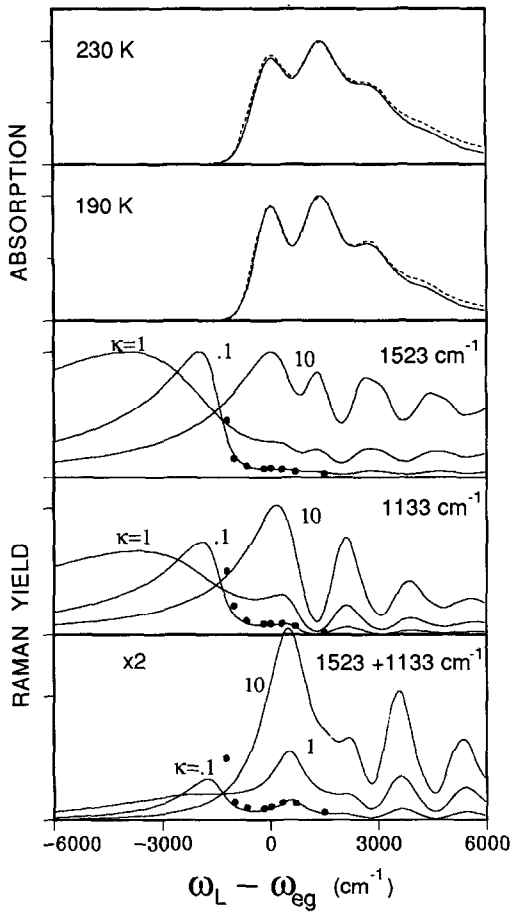

Fig. 1. Top panel: Experimental (dashed curve) and calculated (solid line) (eq. (8)), for the 230 K absorption lineshape of TNBC. Parameters used in the calculation: $d_1 = 1.09$, $d_2 = 1.17$, $\omega_1'' = 1523\ \text{cm}^{-1}$, $\omega_1' = 1625\ \text{cm}^{-1}$, $\omega_2'' = 1133\ \text{cm}^{-1}$, $\omega_2' = 1150\ \text{cm}^{-1}$, $\omega_{eg} = 21320\ \text{cm}^{-1}$, $\gamma^r = 6.5\ \text{cm}^{-1}$, $\gamma^v = 21\ \text{cm}^{-1}$, $\kappa = 0.1$ and $\Gamma_0 = 1090\ \text{cm}^{-1}$ corresponding to $\Delta = 480\ \text{cm}^{-1}$ and $\Lambda = 48\ \text{cm}^{-1}$. Second panel: Same as the top for the 190 K absorption lineshape. $\omega_{eg} = 21150\ \text{cm}^{-1}$. The broadening parameters are $\kappa = 0.1$ and $\Gamma_0 = 960\ \text{cm}^{-1}$ corresponding to $\Delta = 423\ \text{cm}^{-1}$ and $\Lambda = 42.3\ \text{cm}^{-1}$. Other parameters same as in the top panel. Lower three panels: Experimental (solid circles) and calculated (solid line) (eq. (10)). Relative Raman yield at 190 K for the transitions indicated. In each panel, the yield was calculated for $\kappa = 0.1$, 1 and 10 keeping $\Gamma_0 = 960\ \text{cm}^{-1}$. The other parameters are the same as in the second panel. The experimental data were multiplied by an overall scaling factor to best fit the $\kappa = 0.1$ curves.

to κ and the agreement with $\kappa = 0.1$ is clear. It is evident from these calculations that for very large detuning of $\omega_L - \omega_{eg}$, the Raman yield drops, and far off resonance the entire emission consists of the Rayleigh line. This is a consequence of the Condon approximation. Non-Condon corrections will result in a finite Raman yield at

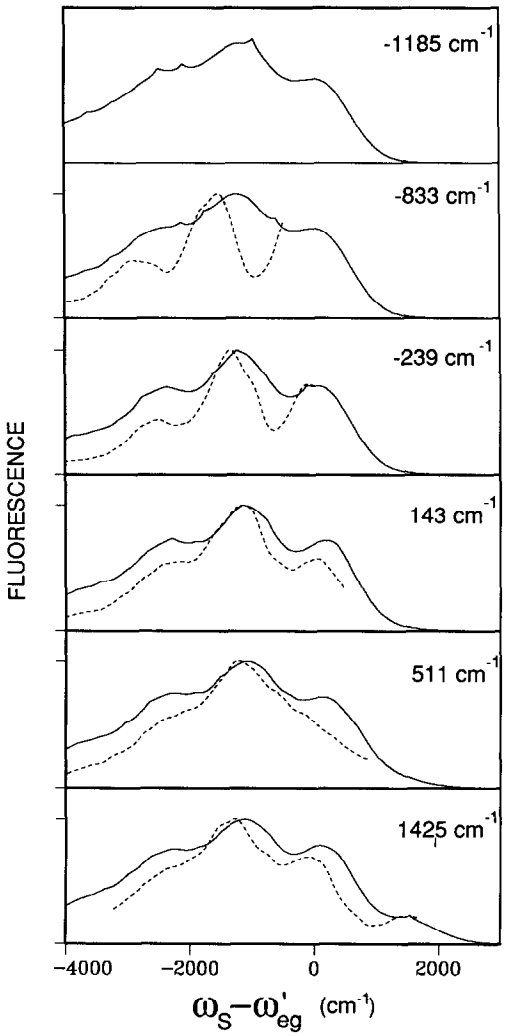

Fig. 2. The fluorescence lineshapes of TNBC at 230 K, dashed curve: experimental, solid line: caleulated using eqs. (7b) and (7d). The various panels correspond to different detunings of $\omega_L - \omega_{eg}$ as indicated, with $\omega_{eg} = 21320$ cm^{-1} and all the lineshapes have been scaled to the same height. The relative intensities of the curves at the maximum peaks for the detunings -833, -239, 143, 511 and 1425 cm^{-1} are 1,5,5,3,3 (experimental) and 1,4,4,3,5 (calculated). Parameters used are the same as for the 230 K absorption (fig. 1) except that $d_1 = 1.31$ and $d_2 = 1.4$. The electronic energy gap for emission, $\omega'_{eg} = 20900$ cm^{-1}, represents a 420 cm^{-1} red-shift relative to the absorption.

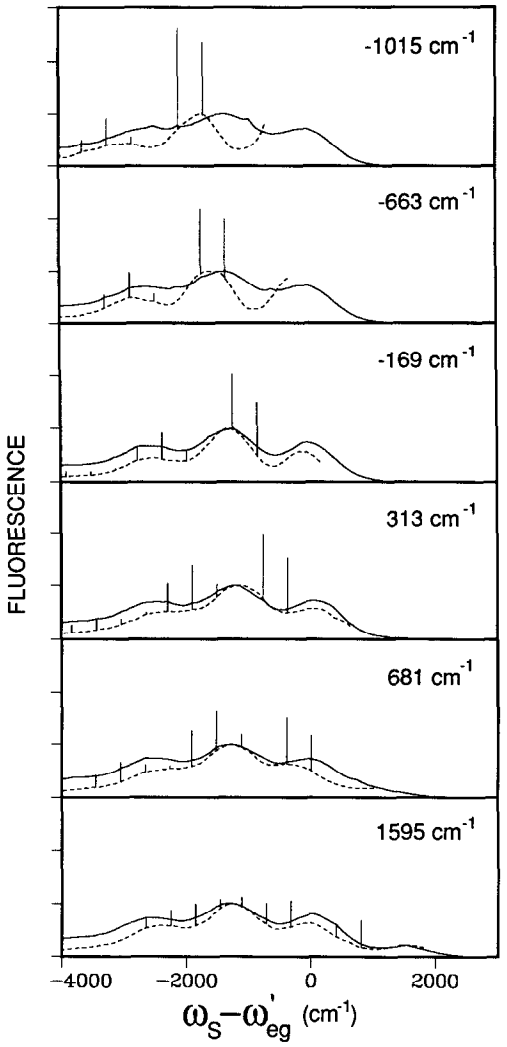

Fig. 3. The fluorescence lineshapes of TNBC at 190 K, dashed curve: experimental, solid line: calculated using eqs. (7b) and (7d). The various panels correspond to different detunings of $\omega_L - \omega_{eg}$ as indicated, with $\omega_{eg} = 21150$ cm^{-1} and all the lineshapes have been scaled to the same height. The relative intensities of the curves at the maximum peaks (from top to bottom) are 1,7,28,17,13,10 (experimental) and 1,5,15,11,10,15 (calculated). Parameters used are the same as for the 190 K absorption (fig. 1) except that $d_1 = 1.31$ and $d_2 = 1.4$. The electronic energy gap for emission, $\omega'_{eg} = 20750$ cm^{-1}, represents a 400 cm^{-1} red-shift relative to the absorption. The experimental Raman lines are included in this figure.

large detuning. The parameters $d_1 = 1.09$ and $d_2 = 1.17$ obtained here are in agreement with a previous fit [5] ($d_1 = 1.0$ and $d_2 = 1.2$) of the Raman excitation profiles. Kinoshita, Watanabe and Kushida [15] recently examined the 0–0 fluorescence peak of β-carotene using a stochastic three-level model and found $\kappa = 0.3$ compared to 0.1 in this case. In a separate analysis of the excitation profiles of β-carotene in polar and non-polar solvents, we have found $\kappa = 0.1$ and that there is only a small amount of additional inhomogeneous broadening [16]. We expect this to hold for TNBC as well.

Fig. 2 shows the experimental (dashed) and calculated (solid line) fluorescence lineshapes for various excitation frequencies at 230 K. The value of detuning, $\omega_L - \omega_{eg}$, is indicated in each panel. For clarity, the sharp Raman lines have been removed from the figure. The relative intensities of the experimental fluorescence spectra in the various panels were calibrated using the solvent line at 2860 cm^{-1} and are given in the caption along with the calculated relative intensities. The best agreement with experiment was obtained by increasing the displacements d_1 and d_2 relative to what we found in the absorption by 20%. In addition we used a different value of the electronic energy gap for the emission (denoted ω'_{eg}) which is red shifted by 420 cm^{-1} with respect to ω_{eg} used in the absorption (fig. 1). These are manifestations of the solvent reorganization process which follows the electronic excitation. Other parameters are identical to those of fig. 1.

In fig. 3 we present similar experimental results and calculations for the fluorescence spectra at 190 K. The experimental intensities for the strongest Raman lines are also shown in this figure. In this case the electronic energy gap for emission ω'_{eg} was red shifted by 400 cm^{-1} relative to ω_{eg} for the corresponding absorption. In both figs. 2 and 3 we were able to reproduce qualitatively the shape of the fluorescence as well as the relative intensity (up to a factor of 2). Our result for $\gamma^v = 21$ is in agreement with ref. [17] and represents a VR rate of 253 fs. The solvent time scale Λ^{-1} is 111 fs at 230 K and 125 fs at 190 K. In order to demonstrate the sensitivity of our analysis to the VR rate, we have plotted in fig. 4 the fluorescence for the $\omega_L - \omega_{eg} = 1595$ cm^{-1} excitation at 190 K for various values of γ^v and γ^r. Haley and Koningstein [17] performed a Raman probe of the S_1 state of β-carotene in CS_2 and found the width of the strong 1524 cm^{-1} fundamental line to be 34 cm^{-1} compared

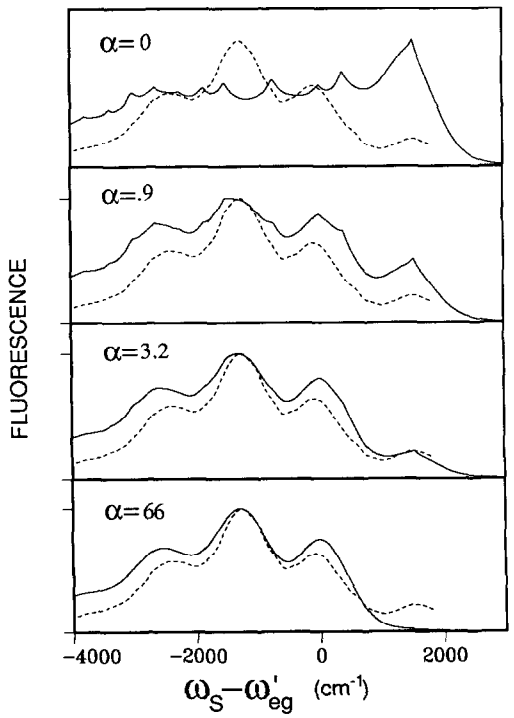

Fig. 4. The fluorescence equations (7b) and (7d) for the 441.6 nm ($\omega_L - \omega_{eg} = 1595$ cm^{-1}) excitation at $T = 190$ K for various values of $\alpha \equiv \gamma^v/\gamma^r$ keeping $2\gamma^r + \gamma^v = 34$ cm^{-1}. Both the calculated (solid lines) and experimental (dashed lines) have been normalized to the same height. The figure demonstrates the sensitivity of the fluorescence lineshape to the VR rate. The best fit $\alpha = 3.2$ was used in figs. 2 and 3.

to 21 cm^{-1} in the S_0 state. Assuming the present relaxation scheme (eqs. (6)) we thus have $2\gamma^r+\gamma^v=34$ cm^{-1} and $\gamma^v=21$ cm^{-1} resulting in $\gamma^r=6.5$ cm^{-1}. These numbers are not expected to be identical in the present study since TNBC lacks the methyl side-groups of β-carotene and consequently has two instead of three Raman modes, and also, the present solvent (isopentane) is different. Nevertheless they provide a rough estimate for γ^r and γ^v. We then varied $\alpha\equiv\gamma^r/\gamma^v$ keeping $2\gamma^r+\gamma^v=34$ cm^{-1}. As α increases the fluorescence tends from unrelaxed (top) to fully relaxed emission (bottom) and the hot band emission from the excited vibronic levels disappear. It is not possible to reduce the hot band intensity and obtain a comparable fit by merely changing the displacements and frequencies. Clearly the dispersed fluorescence is extremely sensitive to α and the best agreement is for $\alpha=3.2$ with $\gamma^v=21$ cm^{-1} and $\gamma^r=6.5$ cm^{-1}. These values were used in figs. 2 and 3. The sharp spikes in the upper panels originate from the broad Raman component and they disappear as α increases.

5. Discussion

In this Letter we presented a detailed experimental and theoretical study of the fluorescence spectra of TNBC in isopentane at 190 and 230 K. Our theoretical analysis of these lineshapes resulted in structural information (molecular frequencies and displacements) as well as dynamical information (the solvent relaxation time Λ^{-}, the solvent coupling strength Δ, and the vibrational relaxation rate γ^v). The value of $\kappa=\Lambda/\Delta=0.1$ implies that the line broadening is in the slow modulation regime. Our agreement for the absorption lineshapes are excellent. The Raman yield shown in fig. 1 provides a sensitive probe for κ and the dispersed fluorescence lineshapes depend crucially on $\alpha\equiv\gamma^v/\gamma^r$, as demonstrated in fig. 4. The agreement between the experimental and the calculated dispersed emission profiles in figs. 2 and 3 is also satisfactory. We were able to reproduce the shape as well as the relative intensities of the dispersed fluorescence.

There are several factors which could contribute to the differences between our calculated and the experimental spectra. First our relaxation matrix which assumes that all vibrational levels relax to the ground state is clearly oversimplified. It is however adequate given the lack of other structural and dynamical information on this system. In addition, non-radiative decay channels (which were not included in the present analysis) will reduce the intensity of the fluorescence. This reduction could depend on the excitation energy $\omega_L-\omega_{eg}$ and will affect the relative intensity of the dispersed fluorescence lineshapes. In addition, we have considered here a single infinite heat bath. This picture is oversimplified. The optically inactive modes of the molecule form a separate finite bath. Vibrational relaxation among these modes is expected to be faster than relaxation to the solvent. This process has been well documented in the work by Kaiser et al. [18] who found a rapid ($\tau<2$ ps) intramolecular VR rate resulting in an increase in the internal temperature of a number of molecules following excitation. The equilibration with the solvent occur on a much longer time scale of tens of picoseconds (e.g. 40 ps for azulene in CCl_4). The resulting VR rate ($(\gamma^v)^{-1}=253$ fs) obtained from our analysis is in accord with the experiments of Weiner and Ippen [18] who measured transient bleaching signals of dye molecules in solution and found, for each dye, a fast transient decay of roughly 70 fs (the pulse width) followed by a long exponential tail with a time scale in the range of 190–480 fs. The decay times were relatively insensitive to choice of solvent and were attributed to intramolecular relaxation processes. The fast transient decay is consistent with our solvent correlation times of ≈ 100 fs. The intramolecular and solvent-induced VR may result in a change in local temperature. These changes are expected to vary with the detuning of $\omega_L-\omega_{eg}$ as different amounts of vibrational energy are available and will affect the resulting line broadening and spectral shifts in the emission. In particular we note that the calculated fluorescence for large negative detuning (-833, -239 for fig. 2 and -1015, -663, -169 in fig. 3) is broader than the experimental. A possible explanation is that for negative detunings we expect vibrational energy to flow from the bath modes to the system modes resulting in an effective cooling of the bath and reduced line broadening.

In conclusion, we have demonstrated how a detailed analysis of the Raman and fluorescence lineshapes allows

us to extract the relevant structural and dynamical parameters of this system. A more detailed study in which the dispersed fluorescence is monitored as a function of time following a pulsed excitation may provide a more complete picture of the solvation and relaxation processes [20,21].

Acknowledgement

The TNBC used in this study was a generous gift from Professor C.H. Eugster of Universität Zürich, Zurich, Switzerland. The support of the National Science Foundation, the Japan Society for the promotion of science, the office of Naval Research, the US Army Research office and the Petroleum Fund, administered by the American Chemical Society, is gratefully acknowledged.

References

[1] W.L. Peticolas and B. Hudson, eds., Proceedings of the Xth Raman Conference, University of Oregon, Eugene (1986).
[2] B.R. Stallard, P.M. Champion, P.R. Collis and A.C. Albrecht, J. Chem. Phys. 78 (1983) 712;
D. Lee, B.R. Stallard, P.M. Champion, P.R. Collis and A.C. Albrecht, J. Phys. Chem. 88 (1984) 6693.
[3] A.B. Myers, R.A. Harris and R.A. Mathies, J. Chem. Phys. 79 (1983) 603;
A.B. Myers, M.O. Trulson and R.A. Mathies, J. Chem. Phys. 83 (1985) 5000;
A.B. Myers, M.O. Trulson, J.A. Pardoen, C. Heeremans, J. Lugtenburg and R.A. Mathies, J. Chem. Phys. 84 (1986) 633.
[4] F. Adar, M. Gouterman and S. Aronowitz, J. Phys. Chem. 80 (1976) 2184.
[5] H. Okamoto, S. Saito, H. Hamaguchi, M. Tasumi and C.H. Eugster, J. Raman Spectry. 15 (1984) 331.
[6] P.F. Williams, D.L. Rousseau and S.H. Dworetsky, Phys. Rev. Letters 32 (1979) 196;
D.L. Rousseau and P.F. Williams, J. Chem. Phys. 64 (1976) 3519.
[7] S. Mukamel, Phys. Rept. 93 (1982) 1; J. Chem. Phys. 82 (1985) 5398; Advan. Chem. Phys., to be published.
[8] W.R. Lambert, P.M. Felker and A.H. Zewail, J. Chem. Phys. 75 (1981) 5958;
C.S. Parmenter, J. Chem. Phys. 86 (1982) 1735.
[9] R.M. Hochstrasser and C.A. Nyi, J. Chem. Phys. 70 (1979) 1112;
J.M. Friedman and R.M. Hochstrasser, Chem. Phys. 6 (1974) 151, 155.
[10] J. Sue, Y.J. Yan and S. Mukamel, J. Chem. Phys. 85 (1986) 462.
[11] H. Hamaguchi, I. Hirada and T. Shimanouchi, Chem. Letters (1974) 1405.
[12] S. Mukamel and R.E. Smalley, J. Chem. Phys. 73 (1980) 4156.
[13] J. Katriel, J. Phys. B3 (1970) 1315.
[14] Y.J. Yan and S. Mukamel, J. Chem. Phys., to be published.
[15] S. Kinoshita, J. Watanabe and T. Kushida, J. Phys. (Paris) 46 (1985) C7-419;
J. Watanabe, S. Kinoshita and T. Kushida, Chem. Phys. Letters 126 (1986) 197.
[16] J. Sue and S. Mukamel, to be published.
[17] L.V. Haley and J.A. Koningstein, Chem. Phys. 77 (1983) 1.
[18] F. Wondrazek, A. Seilmeier and W. Kaiser, Chem. Phys. Letters 104 (1984) 121;
N.H. Gottfried, A. Seilmeier and W. Kaiser, Chem. Phys. Letters 111 (1984) 326;
W. Wild, A. Seilmeier, N.H. Gottfried and W. Kaiser, Chem. Phys. Letters 119 (1985) 259.
[19] A.M. Weiner and E.P. Ippen, Chem. Phys. Letters 114 (1985) 456.
[20] R.F. Loring, Y.J. Yan and S. Mukamel, Chem. Phys. Letters, submitted for publication.
[21] M. Maroncelli, E.W. Castner, S.P. Webb and G.R. Fleming, in: Ultrafast phenomena, Vol. 5, eds. G.R. Fleming and A. Seigman (Springer, Berlin, 1986).